Theses of Doctoral (Ph.D.) Dissertation

QUALITATIVE ASSESSMENT OF *Haemonchus contortus* INFECTION IN SMALL RUMINANT FLOCKS IN HUNGARY: PREVALENCE AND DIAGNOSTIC STUDY

Prepared by:
Rojesh Khangembam
Ph.D. candidate

Dissertation supervisor(s):
Dr. Nóra Pálfyné Vass, *DVM*, *Ph.D.*
Assistant Professor

UNIVERSITY OF DEBRECEN
Doctoral School of Animal Science

Debrecen, 2023

1 INTRODUCTION and AIMS

Haemonchus contortus, which is also commonly known as "Barber's Pole Worm", is an abomasum residing worm that is arguably considered the most pathogenic gastrointestinal nematode (GIN) species infecting small ruminants across the world. The pathogenic effect is due to its voracious blood-sucking nature and also its high fecundity. Hence, haemonchosis is one of the most clinically as well as economically significant parasitic diseases (BESIER et al., 2016; SHEN et al., 2017). The treatment and control of the disease incur huge economic losses to the farmers to the tune of about 436 million Australian Dollars (EMERY et al., 2016), 103 million USD and 46 million USD annually in India and South Africa.

The origin of *H. contortus* is considered to be from Africa then evolved and later propagated elsewhere in the world due to the movement of the host animals and other human interventions (ROSE et al., 2016; SALLÉ et al., 2019). Nowadays, the parasite occurs almost globally and its impact in the European region is also quite significant. There are reports of increasing incidences in the European continent as far as in the colder Scandinavian countries. Yet, there are only very few published reports on the occurrence of haemonchosis in the sheep farming sector in Hungary.

To date, the most common control and treatment method for this parasite is based on anthelmintic drugs. However, for an effective control and treatment program, an accurate diagnosis is being sought, considering the occurrence of mixed infection at the field level. Yet, the accurate differential diagnosis of the parasite is difficult with the commonly employed laboratory microscopy techniques and faecal egg examination (FEC). Also if at all available, the molecular-based techniques are sophisticated, labour-consuming and not suitable for farm-site diagnosis.

This gap in accurate diagnosis by the molecular technique can be filled to some extent with the introduction of isothermal amplification techniques. Among them, the most promising ones are the loop-mediated isothermal amplification (LAMP) and recombinase polymerase amplification (RPA) techniques. There are already available reports of these techniques adopted for the detection of major diseases of plants, humans and animals (OLIVEIRA et al., 2021), either at the research or commercial level. This is also demonstrated in the increase of such isothermal amplification-based test kits for the covid-19 diagnosis. Yet, most of the point-of-care (POC) diagnostics being developed for parasitic diseases are mainly concentrated in the area of parasitoses of humans. Keeping

in view the importance of *H. contortus* in terms of its diagnosis and the very limited data on its prevalence in Hungary, this study has adopted to pursue the following aims:

- Screening of small ruminant farms in and around Eastern and Central Hungary for *H. contortus* parasitism by using faecal egg examination techniques
- Proof of concept development of qualitative LAMP technique for *H. contortus* diagnosis
- Proof of concept development of qualitative and farm-site friendly LAMP-LF technique for *H. contortus* diagnosis
- Proof of concept development of a qualitative and farm-site-friendly RPA technique for *H. contortus* diagnosis

2 MATERIALS AND METHODS

2.1 Sample location, ethics and sources of positive control specimens

The faecal samples used were collected from the animals as per the Hungarian Animal Protection and Welfare Act (Act XXVIII of 1998, 3.§) from farms (n = 14) in six counties in and around Eastern and South-Eastern Hungary between 2019 and 2022 (excluding covid-19 lockdown period in 2020-2021). Additionally, suspected adult *H. contortus* obtained from farmed roe deer (*Capreolus capreolus*) abomasums and also a pooled goat faecal sample were also utilised (assigned as Farm FD and Farm FG, respectively). It should be noted here that the samples were obtained as part of a separate larger study (Toth, unpublished) that dealt with the epidemiology of trichostrongylidae worms. Thus, detailed FEC of the individual animals was outside the scope of this study and hence, only the average FEC of the farms were utilised.

A positive control specimen of *H. contortus* eggs (designated herein as 'KS'), obtained from the abomasal contents of lambs infected orally with approximately 5000 L3 infective was obtained from the Institute of Parasitology, Košice, Slovakia. Another nine species of trichostrongyle worms (*Cooperia curticei, Haemonchus contortus, Nematodirus battus, Oesophagostomum venulosum, Teladorsagia circumcincta, Trichostrongylus axei, Trichostrongylus colubriformis, Trichostrongylus vitrinus* and *Trichuris ovis*) and a batch of pure *H. contortus* eggs were also obtained courtesy of Dr Lynsey Melville, Moredun Research Institute, Scotland. Another positive control gDNA sample (designated herein as BP) was also kindly provided by the Department of Parasitology and Zoology, University of Veterinary Medicine, Budapest.

All the laboratory experiments were performed at the molecular laboratory of the Doctoral School of Animal Science, Institute of Animal Science, University of Debrecen, Hungary. The meteorological data of the above locations were obtained from the Centre for Precision Farming, R&D Services, FAFSEM, University of Debrecen. Some methodological and data analysis parts of the study were also done in collaboration with the School of Veterinary Medicine, University of Glasgow, Scotland.

2.2 Faecal egg examination by Mini-FLOTAC

FEC was performed using saturated sodium chloride solution (specific gravity of 1.200; dilution ratio of 1:10) as the floatation medium, using the Mini-FLOTAC system as per the protocols laid down by CRINGOLI et al., (2010). Briefly, 5g of the faecal sample was loaded using the conical collector and 45 ml of the saturated salt solution was filled in the Fill-FLOTAC. Then, a faecal suspension was prepared by homogenising the

loaded faecal sample with a pumping The Fill-FLOTAC was inverted/shaken and the faecal suspension was charged into both the chambers in the Mini-FLOTAC. After allowing the eggs to be floated for 10 min, the eggs were counted using an Olympus BX51 microscope under 10x. The EPG was calculated by multiplying the counted eggs by a factor of 5. All photographic records were taken using the cellSense software via a DP70 digital camera (Olympus) mounted on the microscope.

2.3 PNA fluorescence microscopy

2.3.1 Faecal egg harvesting/concentration with centrifugation

The eggs were harvested from the faecal solution described above with a slight modification from the protocols reported by ABBAS and HILDRETH, (2019) and JURASEK et al., (2010). Briefly, the remaining Fill-FLOTAC suspension, after charging in the Mini-FLOTAC, was sieved through a 250µm filter sieve (Thermo-Scientific) into a Falcon tube (VWR International) and centrifuged at 1000 x *g* for 2 min. Then, 5 ml of the supernatant was aspirated carefully and transferred to a new Falcon tube. The volume was adjusted to 45ml by adding distilled water. After the final centrifugation at 2000 x *g* for 5 min, the supernatant was discarded without disturbing the pellets. The above steps were replicated twice with the pooled faecal samples of each farm and finally, the pellets were collected in a 2ml tube. A replicate of the pellet was verified for eggs.

2.3.2 Faecal egg harvesting/concentration without centrifugation

Keeping in view the farm-site proof of concept assay design, another centrifuge-free egg concentration method was carried out as described by FRANCIS and ŠLAPETA, (2022) with a modification for Fill-FLOTAC faecal suspension (Figure 1).

Briefly, the faecal suspension after being sieved through the 250µm filter, was divided into four batches of 10ml each in a test tube. After allowing a floatation of 10 min, about 2ml of the upper fluid meniscus was aspirated into a new 2ml. Then, a clean 200µl pipette tip was inverted allowing again the fluid meniscus from the 1.5ml tubes to be aspirated into it by capillary action, with the aim of harvesting/concentrating as many eggs as possible. The egg presence was verified by checking one of the replicates under 10x microscopy.

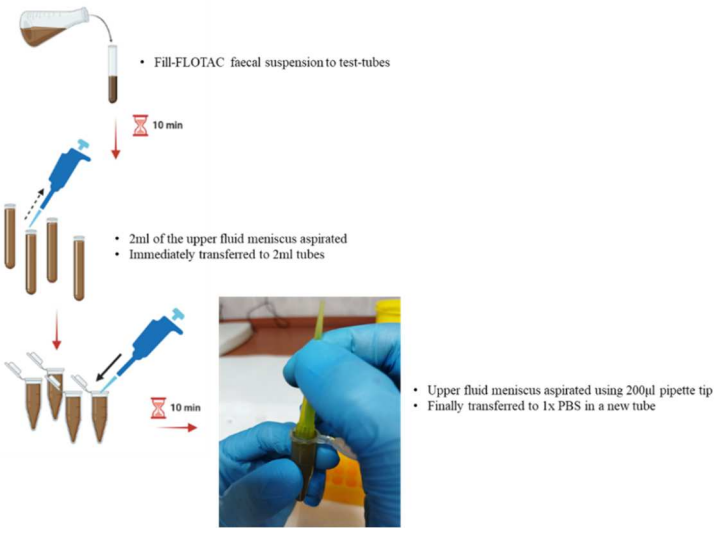

Figure 1: Schematic diagram of egg concentration from Fill-FLOTAC suspension without a centrifugation step. The top fluid meniscus of the faecal suspension was collected in 1.5ml tubes and allowed floatation. The floated eggs were recovered by an inverted 200µl pipette tip.

2.3.3 PNA fluorescence microscopy

This was performed according to the protocols reported by JURASEK et al. (2010) with some modifications. The PNA-FITC (Sigma-Aldrich) was reconstituted at 5µg/ml and aliquoted into individual working 1ml solutions. Then, the reconstituted PNA-FITC aliquot was transferred to the tube containing the egg pellet and incubated for 1 hour under constant agitation at room temperature using a benchtop vortexer in the dark. Then, 15-20µl of the egg sediment was transferred onto a clean glass slide, covered with a coverslip and were examined with a fluorescence microscope using FITC filters (480-490nm excitation filter, Olympus BX51 microscope mounted) in a dimly lit laboratory. The same staining was also performed for the pure *H. contortus* egg culture. Each sample was examined and stained eggs were counted in two technical replicates. Partially stained and unstained eggs were counted as negative results. Again, the photographic records were taken using the Olympus cellSens software through an Olympus DP70 camera mounted to the Olympus BX51 microscope.

2.4 DNA extraction

It should be noted here that for the pooled sample DNA extraction, a minimum of n =5 individual animals were considered. All the DNA quantifications and purity analysis were accomplished using the Synergy HTX Multi-Mode Microplate Reader (BioTek) installed with Gen5 Software (version 3.03, BioTek).

2.4.1 Crude DNA extraction trials

It is to be noted here that the following crude DNA extraction methods were also trialled keeping in line with the POC assays. Wherever centrifugation was necessary, the low *g* centrifuge machine (FVL-2400 Combi-Spin Centrifuge/Vortex (BioSan, Latvia) was used.

Magnetic beads-based method: This was conducted using the commercially available magnetic beads-based genesigEasy DNA/RNA Extraction Kit (Primerdesign Ltd, UK). The positive control sample used here was the KS. Extraction was performed following the protocols described by the kit manual. The farms were arbitrarily chosen for this trail and done in technically replicated.

Glass-bead beating lysis method: This was done as described in MELVILLE et al., (2014) with a slight modification. To each 2 ml tube containing the egg pellets, 200 mg of the glass beads were added and vortexed for 5 min. Finally, the lysate from each replicate was diluted 1:5 with double-distilled water and used as the template per LAMP reaction.

Chelex reagent-based methods: Three sub-trials were performed using Chelex 100 (BioRad) solution-based crude DNA extractions following a few protocols and studies using this chemical for crude DNA extraction (AWAWDEH et al., 2019; GUEVARA et al., 2018). These modified protocols are briefly described in Figure 2.

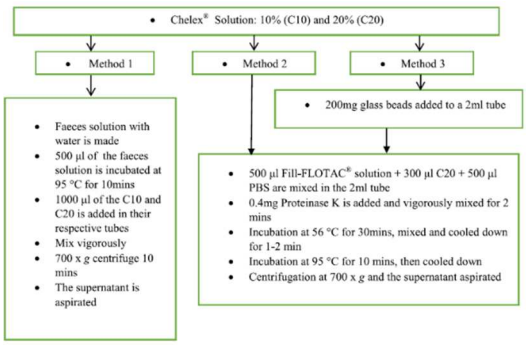

Figure 2: Chelex reagent-based crude DNA extraction.

Motorised micropestle method: For this, the eggs were harvested as described in section 2.3.2. Briefly, the eggs from the topmost film of the faecal suspension were collected in the 1.5ml tube. A battery-operated motorised and micro-pestle compatible Kimble Handheld Homogeniser (VWR, catalogue SCERSP749540-0000) was used to homogenise thoroughly the egg pellets for about 3-5 min. Each sample was done in replicates and care was taken to change the micro-pestle grinder tip for each replicate. After the homogenisation, a small volume of the suspension was observed under the

microscope to verify the egg lysis. Then, this suspension was used as the starting material for the DNA extraction using the genesigEasy DNA/RNA Extraction Kit (Primerdesign Ltd, UK) following the manufacturer's protocol.

2.5 Species-species ITS2 PCR

Species-specific ITS2 PCR for *H. contortus* was performed using a GoTaq Flexi Polymerase PCR kit (Promega), according to the kit manual. The parasite-specific ITS2 primer set used in this study was originally described by REDMAN et al. (2008) and the primers were ordered from Eurofins Genomics. The thermal profile of the PCR was as set: 94 ºC for 2 min for initial denaturation; 35 cycles each of 94 ºC for 30 sec for denaturation; the annealing temperature of 50 ºC for 30 sec and 72 ºC extension for 30 sec, with a final extension step of 72 ºC 10 min. Results were analysed and the records were maintained by using ChemiDoc XRS+ System and Image Lab software (BioRad) after 2% agarose gel electrophoresis with ethidium bromide staining. The amplicon size was 320 bp as per REDMAN et al., (2008). The primer sequence is given in Table 1.

2.6 Colourimetric LAMP

A validated primer set (as given in Table 1) published by MELVILLE et al. (2014) was adopted for the LAMP assay in this study but the method of the end result detection was different from the original study. To facilitate a naked eye detection of the results, a WarmStart Colorimetric LAMP 2X Master Mix (DNA & RNA) with UDG kit (New England Biolabs Ltd, UK) was utilised. The LAMP assay was carried out as defined by the kit manual in a total of 25µl reaction volume. For initial optimisation, the reaction was run using an Alpha Cycler 1 (PCRmax, UK) at temperature-time conditions of 60 ºC to 63 ºC for 30–45 min using the positive control DNA (either BP or KS or both) as well as a non-template control using the molecular grade water during optimisation. All reactions were done in technical replicates. Whenever a visually detectable colourimetric change of orange-yellow happened in the reaction mix, the result was said to be a positive result while the negative result was interpreted by the pink-red colour of the reaction mixture. Once this initial optimisation was established, the assay was replicated successfully using the VWR Advanced Mini Dry Block Heaters (VWR International). To determine the analytical sensitivity of the assay, a 10-fold serial dilution of the positive control DNA was prepared out of which 1µl each of the dilutions was used for the LAMP reaction at 62ºC for 30 min.

Table 1: Primer sequences used in the study. **: primers custom tagged with FITC and Biotin respectively at FIP and BIP for the LAMP-LF assay.

Assay	Primer ID	Sequence (5'- 3')
LAMP and LAMP-LF	FIP**	AACAATCACAGCCGCCACTAAGCTCTATTACATGAGGTGTC
	BIP**	TCATTGATGGTTGAGCTTGAGACTTGTTCGTACTTAACCACCATCA
	F3	GGTTCCATTGATCACGAGAA
	B3	CAGTACACCACATACTCAAGAA
	FLP	AAGCGGCTCATGTCATACAT
	BLP	CTATAATACTGCCTCGCCGTT
ITS2 PCR	Forward	GTTACAATTTCATAACATCACGT
	Backward	TTTACAGTTTGCAGAACTTA
RPA	R_HC-1	Forward : ATATCATTCAGGAATGTTACAATTTCATAA Backward: AACATTCATTTTTACAGTTTGCAGAACTTA
	R_HC-2	Forward : GTTACAATTTCATAACATCACGTTGCATGT Backward: TTACAGTTTGCAGAACTTAGTGTTCACATTC
	R_HC-3	Forward: GTTACAATTTCATAACATCACGT Reverse: TTTACAGTTTGCAGAACTTA

2.6.1 LAMP-LF assay

The HybriDetect-Universal Lateral Flow Assay Kit (Milenia Biotec, Germany) was utilised for the detection of dual-tagged LAMP amplicons. At the 5' ends of FIP and BIP primers, the LAMP primers described above were tagged with fluorescein isothiocyanate (FITC) and biotin (BIO) respectively (Table 1). The LAMP primer concentration and reaction conditions are the same as previously described. The assay optimisation was performed according to the kit manual. The results were recorded after incubation at room temperature at two intervals of 5 and 10 min. The positive result was interpreted only when both the Control and Test bands were stained and the negative result was interpreted if only the Control band was stained as shown in Figure 3.

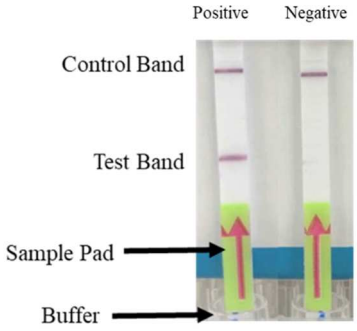

Figure 3: Lateral flow dipstick setup and how to interpret the correct results. Positive results=when both the Control band and the Test band showed colour; Negative results = when the Control band showed colour.

2.7 RPA technique

2.7.1 RPA primer design and primer screening

Briefly, ITS2 nucleotide sequences of *H. contortus* were obtained from the Genbank (https://www.ncbi.nlm.nih.gov/genbank/) and pairwise aligned adopting the MUSCLE alignment algorithm (with a minimum of 8 iterations). Then, the PCR primer sequences as described earlier were annotated to the aligned consensus sequence. The annotated sequence was modified to increase the length of the primer as per the conditions as stated by the TwistDx manual for RPA primers. Finally, two pairs of custom-designed RPA primers were selected and ordered for production from Eurofins (Eurofins Genomics, Germany).

2.7.2 RPA reaction and optimisation

The RPA assay was done with each single reaction volume of 50µl utilising the TwistAmp™ Basic kit (TwistDx, UK) as per the kit manual. Betaine (Thermo Scientific) was added in the reaction, as a modification from the manual, to reduce non-specific amplification as per LUO et al., (2019). The incubation conditions were achieved using the same portable heat block (VWR™ Advanced Mini Dry Block Heater). For the optimisation, the RPA amplicons were cleaned using either EXOCleanUp FAST kit (VWR) or ChargeSwitch™ PCR Clean-Up kit (Thermo Scientific) according to the respective kit protocols although results were also analysed without this post-amplification clean-up. Analytical sensitivity was calculated by performing the reaction using a 10-fold serial dilution of the MD positive control DNA template.

2.7.3 Visualisation of RPA reaction by agarose gel electrophoresis

The visualisation of the results of RPA was done by 2.5% gel electrophoresis stained with ethidium bromide using the ChemiDoc XRS+ System and Image Lab software (BioRad). For comparison purposes, the amplicons were also analysed without the recommended post-amplification clean-up step. The amplicon band was 320 bp.

2.7.4 RPA end-point detection using a UV lamp and DNA intercalating dye

This was done as per the protocol initially described by SRISRATTAKARN et al., (2020) with some slight modifications, especially the use of different dyes and the mode of visualisation. Briefly, the RPA amplicon tubes were mixed with 5x EvaGreen® Dye (Biotium) at a 4:1 ratio in technical triplicates. Then, to visualise and interpret the result, the reaction tubes were illuminated by UV rays using the ChemiDoc XRS+ System (BioRad). Similarly, the 10000x GelRed™ (Biotium) at different working concentrations of 10x, 100x, 200x and 300x and in technical triplicates were tested.

2.8 Gene sequencing through Eurofins

Three PCR amplicons using DNA templates of *H. contortus* of Hungarian isolates (F10, F11 and F13) were submitted to TubeSeq gene sanger-sequencing service (Eurofins Genomics). The results obtained were analysed using the Molecular Evolutionary Genetics Analysis (MEGA) version X software as per described by KUMAR et al., (2018). All the sequences were aligned using the ClustalW alignment algorithm and a phylogenetic tree was constructed using the recommended Neighbour-Joining method with the bootstrap value set at 1000.

3 RESULTS

3.1 Microscopy Results

3.1.1 Microscopy: adult worms and eggs

Initially, all the faecal samples were examined under normal microscopy and those farms with high FEC and with suspected *H. contortus* eggs were kept for further downstream analysis. The adult worm specimens obtained from the abomasum of farm FD was also observed under microscopy and identified to be *H. contortus* following the criteria laid down in TAYLOR et al., (2015). The photographic records of the morphological identification of the adult worms are presented in Figure 4. Grossly, the suspected worm specimen presented either reddish or red-white striped and thread-like. The length of the identified adult males ranged from 9-18 mm while those of identified adult females ranged from 15-27mm. The nematode body was observed to be filiform and tapered from the anterior end (Figure 4-A). The anterior end presented a buccal capsule with a noticeable tooth or 'lancet' protruding from the dorsal wall (Figure 4- B). Another striking morphological observation was the longitudinal striations on the body which is termed 'synlophe' (Figure 4 – C). The synlophe can also add to species differentiation as AMARANTE (2011) noted that these structures could extend significantly beyond the midbody in *H. contortus*.

As seen in Figure 4-A, the black arrow shows the cervical papillae, observed at two different magnifications. These cuticular modifications are very prominent in the case of *H. contortus* and positioned from the anterior end about thrice the diameter between papillae. The cervical papillae are often spinous in nature (SOULSBY, 1968; M. A. TAYLOR et al., 2015). Trichostrongyle nematodes are unisexual and so male and female worms are usually presented with distinguishing morphological features. Typically, the adult *H. contortus* females have a vulval flap which is linguiform in shape (Figure 4-B).

While in males, a well-developed bursa that serves copulatory functions is typically unequal in shape and size and also possesses a pair of barbed spicules (Figure 4-C).

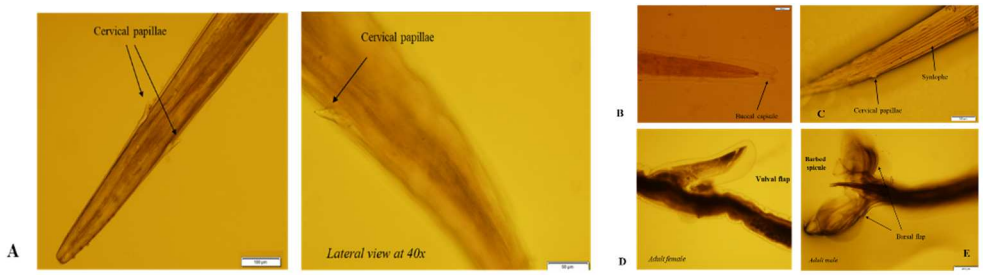

Figure 4: Light microscopy result of adult *H. contortus*. A: anterior end showing the cervical papillae B: buccal capsule; C: 'synlophe'; D: vulval flap in females; D: bursal in males

Some selected photographic records of the commonly encountered parasite eggs in the routine FEC examination are shown in Figure 5. As discussed earlier, only the eggs of *N. battus* can be easily identified due to their reasonably large size and oval-shaped egg with an embryo inside (Figure 5-B). The other most commonly encountered parasite in the study was the Strongyloides worm, which could be observed as larvated eggs (Figure 5-A). Interestingly, a certain number of individual samples (n=84) presented suspected tapeworm species (Figure 5-A, denoted as 'TW') as well as suspected coccidian ova (Figure 5-E, denoted as 'CX'). The tapeworm species is highly suspected to be of *Moniezia* spp, characterised by its distinctive triangular-shaped egg with thick walls and the slightly visible pyriform apparatus inside it. The average dimension of all the samples analysed ranged from 39-43µm in width and 68-89µm in length. The eggshell was observed to be thin, ovoid, slightly yellowish and contained blastomeres inside it. The blastomeres could be either distinctively organised as well as observed to be distributed fully inside the egg (Figure 5 D-E). It should also be noted that certain artefacts (Figure 5-E) were also observed in many of the samples. These artefacts could consist of pollen materials, semi-digested feed particles and air bubbles.

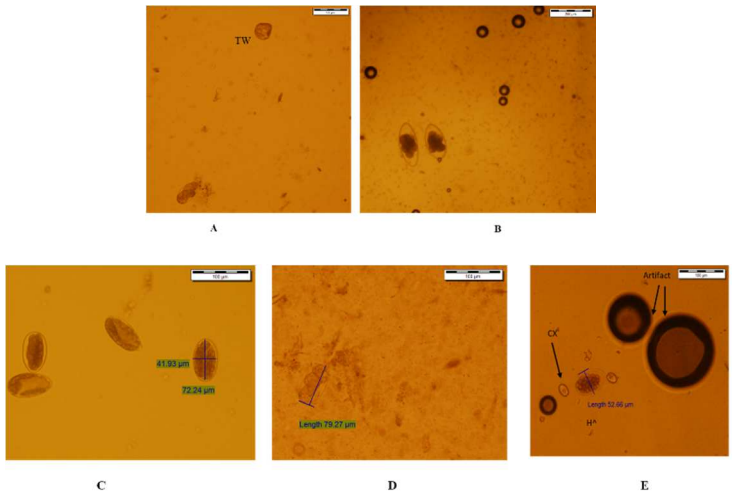

Figure 5: Light microscopy result of parasite eggs observed in routine FEC examination. A: suspected tapeworm (TW) and a Strongyloides; B: *N. battus* egg; C: morphometry of *H. contortus* eggs; D: *H. contortus* from a farm sample; E: artefacts and mixed parasite eggs from a farm sample.

3.1.2 PNA fluorescence microscopy

Those samples suspected to have *H. contortus* from the initial FEC examination were processed for PNA fluorescence microscopy of which the result is shown in Figure 6 (for positive control specimens) and Figure 7 (for farm samples). Positive *H. contortus* eggs were visualised as bright-green stained outlines with some degree of fluorescence stain inside the eggs also (PALMER and McCOMBE, 1996). Figures 6-A and B show UV-illuminated and normal light modes of the same field of view of the positive control eggs with the blastomeres well-filled inside the eggs while Figures 6-C and D show an egg with a clearly defined blastomere. In both these panels, the outline of the eggs was stained in bright green and the blastomeres/embryo also took up the stain. Notably, under the normal light field of view, Figure 6-D could have been 'easier' to be scored as more *H. contortus* egg-like as per many literature and images available for *H. contortus* egg. For instance, SOULSBY (1968) noted that *H. contortus* eggs generally have 16-32 cell stage embryos. This is just a thumb rule and not all eggs of this parasite can be easily differentiated based on the number of cells. The finding of this study also confirmed this, as shown in Figures 6-A and Figures 10-E and F. Here, the embryos also took up the stain slightly but the number of cells could not be counted as easily. The normal light field of view of the same specimen could have been at best identified as 'trichostrongyle/strongylid- eggs' but PNA fluorescence confirmed this as *H. contortus* eggs. The finding reported here is also consistent with that of other PNA fluorescence studies (DOUANNE et al., 2019; JURASEK et al., 2010).

The results of this technique for eggs recovered from farm samples are presented in Figure 7. Interestingly, several eggs that could be marked as *H. contortus* based on the forms/shapes of the blastomeres under normal light were non-*Haemonchus* actually, as seen in Figures 7-A and B. Also, farm samples were usually found with mixed infections. Yet, PNA can effectively discriminate against this. For example, a suspected tapeworm (TW) egg and another trichostrongylid egg (red arrow) are shown in Figure 7- C and D. Although COLDITZ et al., (2002) noted that *Moniezia* spp could take up a slight stain, the suspected tapeworm of *Moniezia* spp (TW) did not take up any stain while the trichostrongylid egg took up a faint stain with an unclear outline (Figure 7 C). At times, larvated/embryonated *H. contortus* eggs could also be detected (Figure 7 G and H) and could be misdiagnosed as a *Strongyloides* spp egg (Figure 7 E-F). Figure 7-I (at 10x magnification) shows a field of view of a mixed infection presenting two *H. contortus* eggs as well as another strongylid egg (red circle).

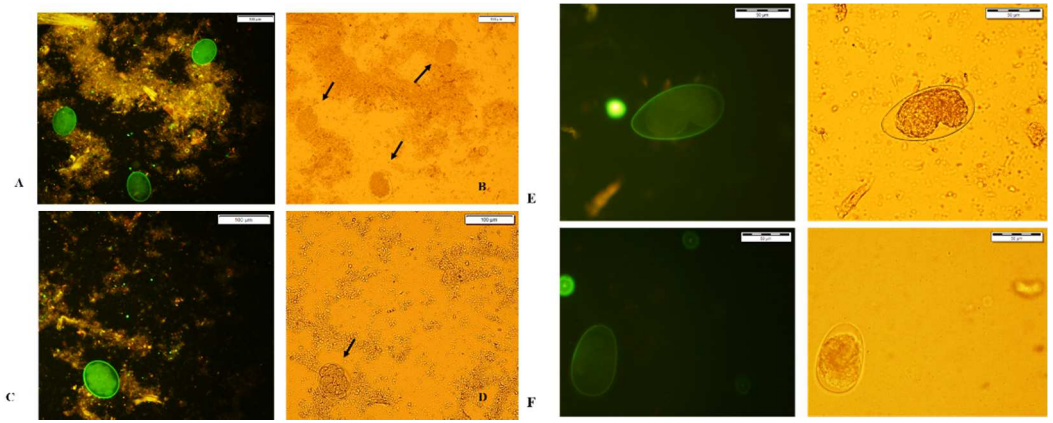

Figure 6: PNA fluorescence microscopy results of the positive control *H. contortus* eggs. The positive result is characterised by a bright green and clearly stained outline of the eggs. Left-side of each panel shows the UV-illuminated field of view while the right side shows the normal light field of view of the same specimen; A-B: blastomeres can be seen filling up inside the egg; C-D: very well-defined blastomeres with visibly countable dividing cells; E-F: 40x magnified view of *H.contortus* egg stained with PNA; Black arrows show the egg positions.

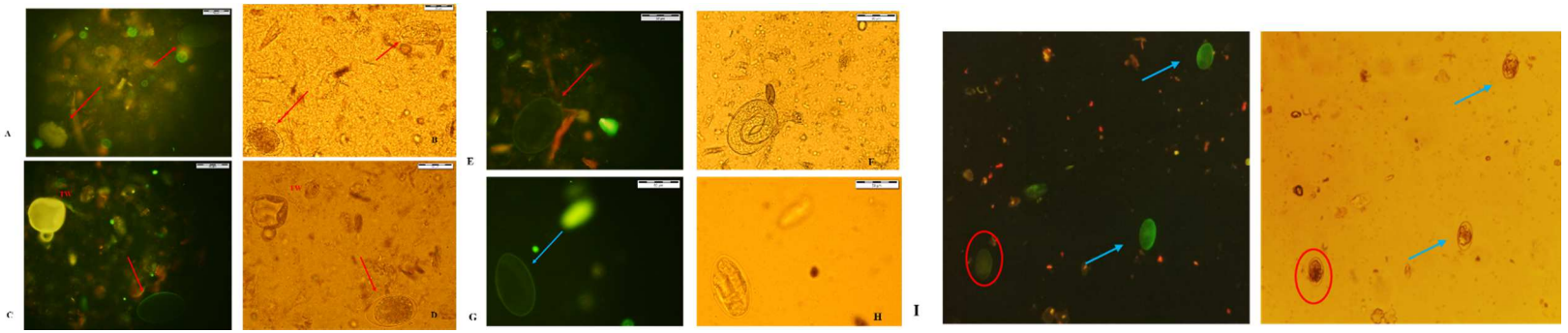

Figure 7: PNA fluorescence microscopy of farm samples. The positive result is characterised by a bright green and clearly stained outline of the eggs. Left-side of each panel shows the UV-illuminated field of view A-B: suspected *H. contortus* eggs under normal light but found to be negative under PNA fluorescence microscopy; C-D: a tapeworm (TW) egg and a trichostrongyle-egg; E-F: *Strongyloides* spp egg that did not stain; G-H: a 'larvated' *H. contortus* egg taking up the stain; Blue arrow = larvated eggs; Red-arrow and red-circle= negative eggs.

3.2 Farm location, meteorological data and brief prevalence report

The farms involved in this study are shown in Figure 8 and designated as F-1 to F-14, and a pooled faecal sample from a goat farm (FG) and adult worms from the abomasum of roe deers (*Capreolus capreolus*) from location FD were also collected. The positive control specimens were obtained from three sources, namely the Department of Zoology and Parasitology, University of Veterinary Medicine, Budapest, Hungary; Institute of Parasitology, Kosice, Slovakia and the Moredun Research Institute, Scotland

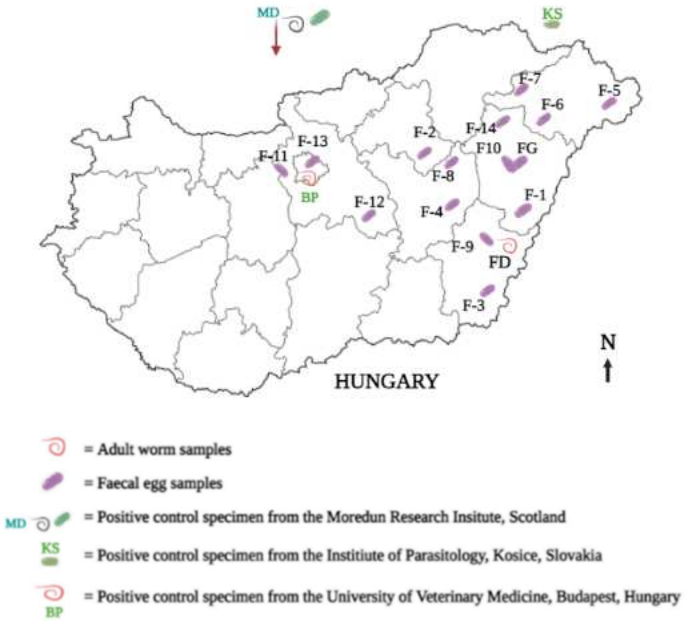

Figure 8: Location of farms covered in the study. F-1 to F-14: sheep farms; FD: roe deer farm; FG: goat farm; MD, BP and KS were sources of positive control specimens.

As mentioned earlier, only the average FEC data of the farms are shown in Table 2. It should be noted that the sampling of farms F-1 to F-9 were done from Autumn-Winter 2018 and in Spring 2019 while F-10 to F-14 were done during the Spring and Autumn of 2021-2022.

Among the fourteen farms covered in the study for FEC examination, F-5 registered the highest average of FEC (= 1750 EPG) and F-6 recorded the lowest average FEC (= 5.7 EPG). It should be noted that F-1 already had a confirmatory diagnosis of haemonchosis by an independent veterinary laboratory as reported by the farmer. As expected, the farm had a positive result in our subsequent assays. F-6 and F-14 (FEC = 22.2 EPG) did not detect any *H. contortus* eggs. Interestingly, F-5, F-8 and F-12 all detected a high number of other parasite species eggs, especially tapeworm (and *Coccidia* spp. up to some extent). Also, the degree of intensity of the farms is shown in Table 2 as

per the intensity of FEC interpretation criteria laid down by TAYLOR et al., (2015) for mixed infection in small ruminants. The study also attempted to analyse if the climatic conditions of the farms have any relation with the FEC output, especially of *H. contortus* eggs. For this, only the farms F-1 to F-9 were utilised as the data collection was done more uniformly within two seasons while the other farms could not be uniformly collected due to the covid-19 pandemic. The FEC was compared against the average temperature, cumulative rainfall and average relative humidity. It was found that there was no significant correlation between the average temperature and the mean FEC vs average temperature (p=0.2), FEC vs relative humidity(p=0.26) and FEC vs Rainfall (p=0.86).

Table 2: Average FEC of the sheep farms involved in the study and degree of infestation as per TAYLOR et al., (2015); Light: <250 EPG; Moderate: 1000 EPG; Heavy: +2000 EPG.

Farm ID	Average FEC (in EPG)	Degree of Infestation	Remarks
F-1	600	Moderate+	The farmer already reported positive haemonchosis
F-2	150	Light	
F-3	276.4	Moderate	
F-4	982.2	Moderate+	
F-5	1750	Moderate++	Mixed infection with other parasite families
F-6	5.7	Light	Negative for *H. contortus*
F-7	113.7	Light	
F-8	767.2	Moderate+	Mixed infection with other parasite families
F-9	168.0	Light	
F-10	159.7	Light	
F-11	577.1	Moderate	
F-12	754.2	Moderate+	Mixed infection with other parasite families
F-13	70.9	Light	
F-14	22.2	Light	Negative for *H. contortus*

Temperature and moisture conditions are the prevailing factors which impact the free-living stages of *H. contortus.* Also, the duration of the life cycle is reliant on temperature, with the developmental rate growing at warmer temperatures. Also, the phenomenon of hypobiosis during unfavourable environmental conditions also greatly affects the maturating and subsequent faecal egg shedding (O'CONNOR et al., 2006; TAYLOR et al., 2015; BESIER et al., 2016b). The finding of this study showed no significant correlation between the analysed meteorological data and the FEC. This could

be due to hypobiosis and also the locations shared similar weather traits. Further in-depth meteorological analysis along with the spatial distribution pattern study is warranted.

3.3 LAMP assay

3.3.1 Optimisation, analytical sensitivity analytical specificity

Initial optimisation of the LAMP assay was performed to define the optimal temperature for the reaction using and the result is shown in Figure 9. Although amplification was detected in all the temperature ranges (Figure 9-A) described in section 2.6, subsequent analysis was adopted at 62ºC arbitrarily. Also, the assay was initially run for a maximum of 45 min although subsequently, a 30 min reaction time was determined to be acceptable. For visual detection, the positive result was interpreted as a colourimetric change from pink/purple to yellow/orange as specified in the kit manual

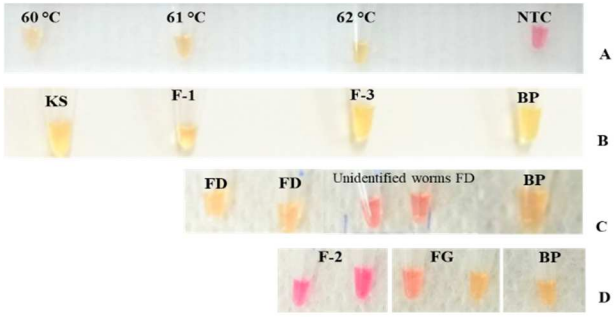

Figure 9: Optimisation of LAMP assay. NTC: non-template control; BP: positive control template from Budapest; KS: positive control; F1-F3 and FD-FG: farm sample. NTC: Non-template control; Pink/Purple = Negative; Yellow/Orange = Positive.

To verify the result of the arbitrarily chosen temperature-time combination described above, LAMP assay was also performed using farm samples F-1 and F3 and a positive result was detected (Figure 9-B). Furthermore, gDNA extracted from the suspected *H. contortus* adult worms, obtained from the abomasum at post-mortem from a farmed deer (Farm FD), showed positive results while the gDNA samples of a few unidentified worms collected from the same FD were found to be negative (Figure 9-C). Similarly, faecal samples from goats (Farm FG) were found positive (Figure 9-C). However, pooled faecal samples (Farm F-2) of individual sheep with no trichostrongyle egg counts observed during FEC gave negative results (Figure 9-D).

The detection range of the assay was found to be 2.5 x 10^{-1} ng/µl to 2.5 x 10^{-4} ng/µl based on the 10-fold serially diluted BP positive control template LAMP assay (Figure 10). The sensitivity of our assay was also found to be close to that of MELVILLE et al., (2014) which reported a minimum detection limit of '10^{-5} ng/µl' of serially diluted positive control gDNA. The minor decrease in the sensitivity of LAMP in this study

compared to that of the original study (MELVILLE et al., 2014) could be justified by the difference in the end-result detection system. Whereas the original study employed the UV illumination technique, this study LAMP assay simply relied on naked-eye detection of colourimetric change. Yet, this colourimetric detection offers the advantage of minimal equipment usage for a POC diagnosis system.

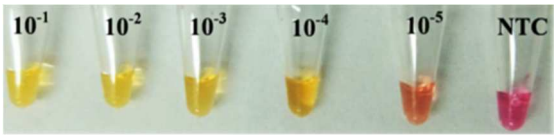

Figure 10: Analytical sensitivity of the colourimetric LAMP assay. NTC: non-template control. Pink/Purple = Negative; Yellow/Orange = Positive

For specificity analysis, nine positive control specimen worms of the trichostrongylidae family were used as the template gDNA for the LAMP assay and the result is shown in Figure 11. As anticipated, only the gDNA of the *H. contortus* showed a colour change to yellow-orange meaning a positive result (Figure 11-B lower panel). Whereas, the other eight species showed shades of pink-purple that are nevertheless significantly differentiated from the positive result colourimetric value (Figure 11-B upper panel). To further prove this, the single-species ITS2-PCR showed the same result (Figure 11-A). This study expanded the scope of this original study by utilising a commercially available colourimetric kit adaptable for a naked eye detection system. level.

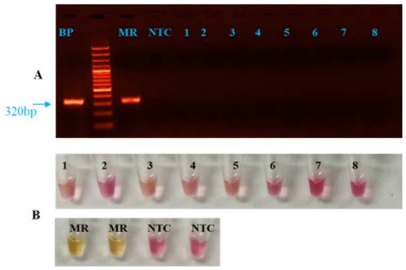

Figure 11: Specificity validation of the LAMP assay using the nine positive control parasite specimen from the Moredun Research Institute. A: ITS2 PCR result. 100bp ladder; B: LAMP assay using the same gDNA. 1 = *N. battus,* 2 = *T. axei;* 3 = *T. vitrinus;* 4 = *T. colubriformis;* 5 = *T. circumcincta;* 6 = *O. venulosum;*7 = *T. ovis;* 8 = *C. curticei*; MR: Moredun positive control; NTC: Non-template control; Pink/Purple = Negative; Yellow/Orange = Positive

Thus, after adequate optimisation, the LAMP assay was adopted for the subsequent validation with ITS2 PCR and further farm sample trials as described later on. Later on, the assay was performed using the WarmStart® Colorimetric LAMP 2x Master Mix with UDG. Using this kit containing uracil-DNA glycosylase reduced any carryover

contamination and subsequently minimised the risk of false positive results as LAMP amplicons are highly stable and difficult to decontaminate.

3.3.2 Individual and pooled sample LAMP assay

As a followed up on the above results, the assay was tested more by expanding the sample size and also including samples from individual sheep as well as pooled samples. This was done with the objective to verify the assay's diagnostic sensitivity for individuals as well as flocks. The result of this is shown in Figure 12. There are already reports validating the necessity as well as the advantage of pooled faecal sampling for parasitic disease detection (PARAS et al., 2018; RINALDI et al., 2019).

Farm F-4 faecal samples recorded a very high trichostrongyle FEC (Table 4) with some individual samples suspected of having *H. contortus* eggs. LAMP assay using these individual samples as well as pooled samples detected positive results (Figure 12A-B). Faecal samples from Farm F-6 were already found to have a very low average egg count (EPG = 5.96) and no detectable trichostrongyle eggs by microscopic analysis (Toth et al., unpublished). The LAMP analysis of randomly selected individual samples of F-6 was found to have negative results (Figure 12-C). Similarly, pooled and individual samples were examined from Farm F-8 and tested positive (Figure 12-D).

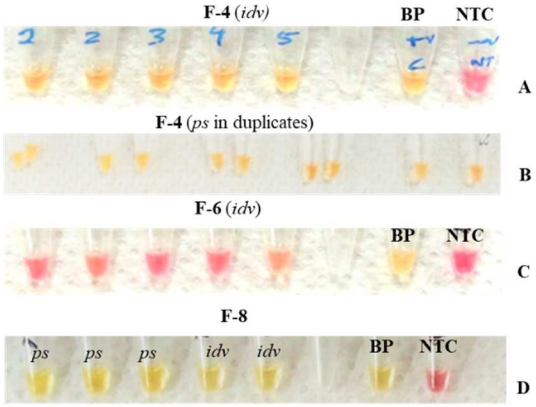

Figure 12: LAMP assay using the individual as well as pooled faecal samples. F-4 to F-8: farm gDNA; *idv*: individual sample; *ps*: pooled sample.

3.3.3 ITS2 single-species PCR validation

Following the predicted detection of *H. contortus* in some farms mentioned above, ITS2 single-species PCR was performed to validate the LAMP assay and the result is shown in Figure 13. Farms F-1 to F5; F-7 to F-13; FD and FG were all recorded to have positive results while farms F-6 and F-14 recorded negative results in both the PCR and LAMP. None of the controls used showed false results.

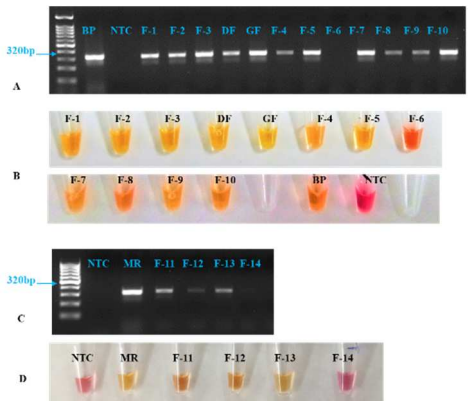

Figure 13: Single-species ITS2 PCR validation of the LAMP assay. A-C: ITS2 PCR result. 100bp ladder; B-D: LAMP assay; BP: Budapest control; MR: Moredun control; NTC: Non-template control; Pink/Purple = Negative; Yellow/Orange = Positive

3.4 Crude DNA extraction trials

For the Chelex® reagent-based methods, no positive LAMP results were obtained. Also, the KS samples for Chelex® Method 1 could not yield any reading as the analyte was not clear enough for the absorbance reading.

The magnetic bead extraction protocol gave inconsistent LAMP results. One replicate of the positive sample KS showed a negative result (Figure 14-A). Yet, both replicates from Farm F-4 showed positive results while that of Farm F-6 showed negative results, as expected (Figure 14-A).

For the bead-beating technique, the supernatant from the direct Fill-FLOTAC solution did not yield any positive results by LAMP (Figure 14-B). However, the protocol was slightly modified by using the benchtop low *g* centrifuge machine. This led to an improvement in the detection of *H. contortus* DNA as two out of three technical replicates gave positive LAMP results (Figure 14-C).

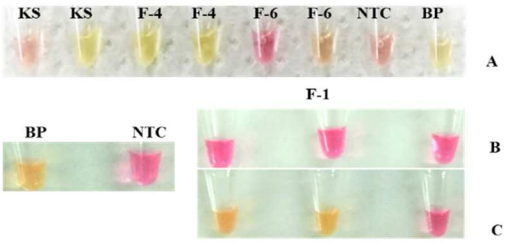

Figure 14: LAMP assay for crude DNA extraction. BP, KS: positive control; F-1 to F-6: farm samples. NTC: Non-template control;Pink/Purple = Negative;Yellow/Orange = Positive.

For the micropestle-crude DNA extraction method, microscopic analysis of the suspension after the application of the micro-pestle action showed the breaking of

eggshells (Figure 15 – C) and PCR analysis of the subsequently extracted DNA yielded positive results (Figure 15-B).

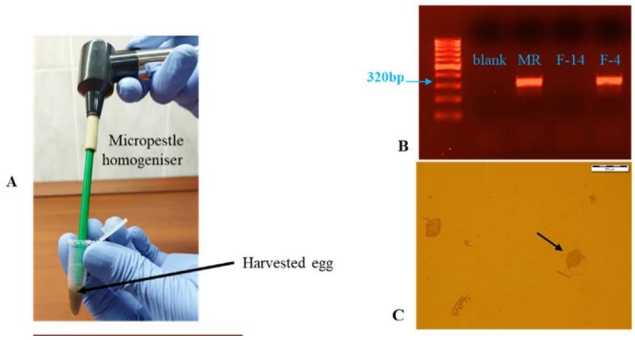

Figure 15: Micropestle homogeniser crude DNA extraction. A: Micropestle application.; B: ITS2 PCR; C: Photo of a broken eggshell (arrow). MR: positive control; Blank: control tube with no eggs. F-4, F-14:positive and negative farm samples

3.5 LAMP-LF Assay

3.5.1 LAMP-LF optimisation

The initial optimisation was carried out using two *H. contortus* positive control gDNA (BP and KS) and non-template controls. Results showed that the LAMP-LF was capable of detecting these two positive control gDNA samples with no false-positive bands visible for the non-template control (Figure 16-A).

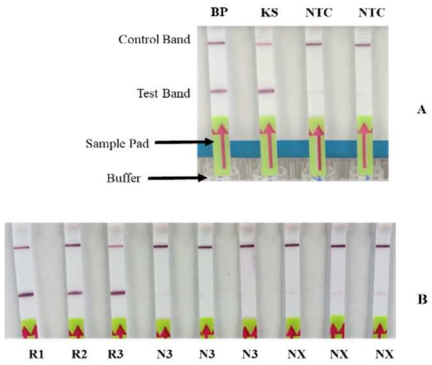

Figure 16: Optimisation of LAMP-LF assay. A: assay result interpretation; B: optimisation of amplicon volume to prevent false positives. BP and KS: positive control templates; R1-R3: LAMP-LF with a positive control template at various amplicon dilutions where R3 being optimised at 1:9 amplicon:ddH_20; NTC, N3-NX: non-template controls.

3.5.2 LAMP-LF field trials

The LAMP-LF was tested in field samples (Table 4) previously predicted to be positive for *H. contortus* by LAMP and confirmed by PCR. The study found 100% agreement between the results of our colourimetric LAMP assay and the LAMP-LF assay, indicating the validity of either of the endpoint detection methods for potential future POC confirmatory diagnosis of *H. contortus*. The results are shown in Figure 17.

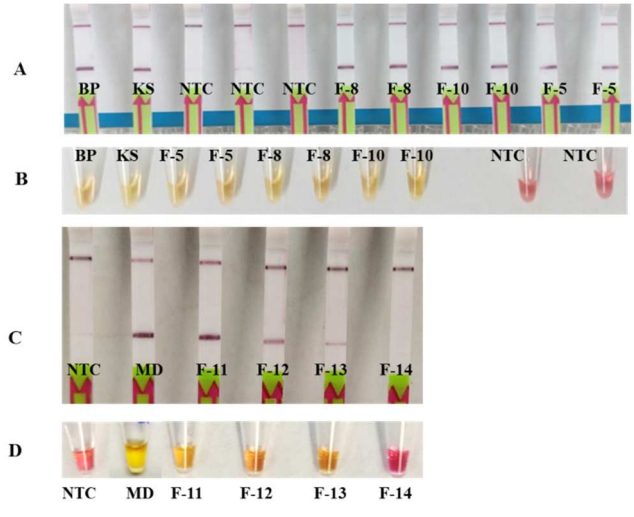

Figure 17: Field trial of some randomly selected farms for LAMP-LF assay. A: LAMP-LF assay using positive control. B: corresponding LAMP assay for farms F-5, F-8 and F-10; C: LAMP-LF assay using positive control from Moredun; D: corresponding LAMP assay for farms F-11 to F-14;NTC: Non-template control;Pink/Purple = Negative;Yellow/Orange = Positive

3.6 4.6 RPA technique

3.6.1 Optimisation: primer, betaine treatment, amplificon clean-up

The RPA reaction time-temperature combination was optimised at 37ºC for 25 min amplification step and a final 85ºC for 5 min amplification termination step. Initially, three primer sets (Table 1) were tried to find out the best fit for the assay. The result of the primer optimisation is shown in Figure 18 (A and B). It can be seen here that the best set of primers is P2 (Figure 18-A) with the least unwanted amplification bands while the other two sets (P1 and P3) gave some unwanted amplification despite the target amplification also being clearly visible. The integrity of this screening could be verified as the kit-positive control bands were distinctly recorded in duplicates.

Once the primer set has been established, the study further aimed to investigate the effectiveness of betaine addition to the two post-amplification kits and the result can be seen in Figures 17-C and D. This post-amplification was recommended by the kit manual for better end-result visualisation. The ChargeSwitch™ PCR Clean-Up kit took longer to perform compared to the enzymatic-based clean-up principle of the VWR ExoCleanUP FAST kit (about 20-25 min and 8-15 min respectively for 8 reaction tubes) although the latter kit gave smearing. The non-specific amplifications observed previously were not detected following the addition of betaine 200 (optimised at 0.8M concentration) in the RPA master mix, as shown in Figure 18-D. This indicates that betaine addition increased

primer specificity as reported in many studies (LOBATO and O'SULLIVAN, 2018; LUO et al., 2019).

Keeping in view POC amenability, the study also attempted to eliminate this post-amplification clean-up and visualised the amplification result without this step using farm F-4 and F-14 as the negative control template and MD as the positive control template. There was no significant difference in the detection of the amplification bands apart from a faintly visible smear track, as shown in Figure 18-D. This could greatly reduce the time to result for future RPA techniques.

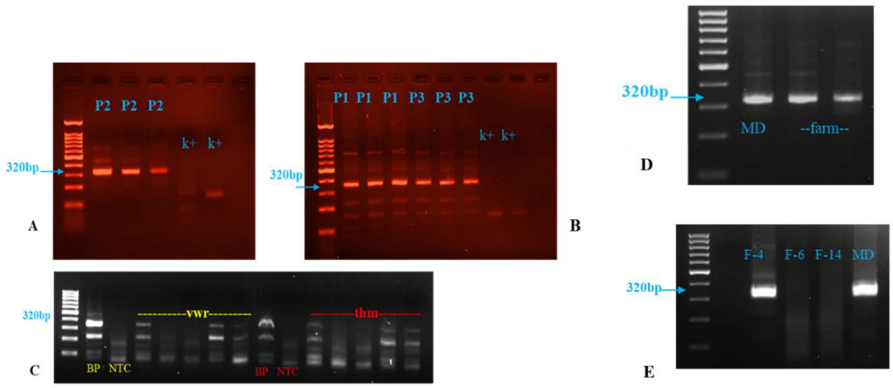

Figure 18: Result of the optimisation of the RPA technique. 100bp ladder used. A and B: Primer screening where P1-P3 are the three primer sets; C: post-amplification result of two different kits; D: Betaine addition trial; E: result without the post-amplification clean-up step; k+: kit positive control; thm: ChargeSwitch™ PCR Clean-Up kit (Thermo-Scientific); vwr: EXOCleanUp FAST kit (VWR); BP: positive control template; NTC: non-template control

3.6.2 Analytical specificity and sensitivity

Amplification was detected at the expected size for *H. contortus* (Figure 19-A) of 320bp. No amplification was seen for any of the remaining species assayed. The specificity of the assay was also verified by the single species ITS2 PCR (Figure 19-B) to confirm species specificity. Only the *H. contortus* template gave a clear band at the expected amplicon size of 320bp for the PCR also. Thus, the RPA assay was in agreement with the result of the single species ITS2 PCR, with no amplification detected in any species other than *H. contortus*. Following confirmation of species-specific amplification, the limit of detection of the assay was established by using a 10-fold serial dilution of positive control *H. contortus* DNA from Moredun. The limit of detection of the RPA assay for *H. contortus* was determined to be 0.1 ng/µl (Figure 19-C). This is lower than that reported for the previous LAMP study the study built upon for this assay, where the limit of detection was between 1 x 10^{-5} ng/µl (MELVILLE et al., 2014) to 2.5 x 10^{-4} ng/µl (KHANGEMBAM et al., 2021). A previous RPA study also reported a limit of detection of 100 fg of *H. contortus* DNA (WU et al., 2021).

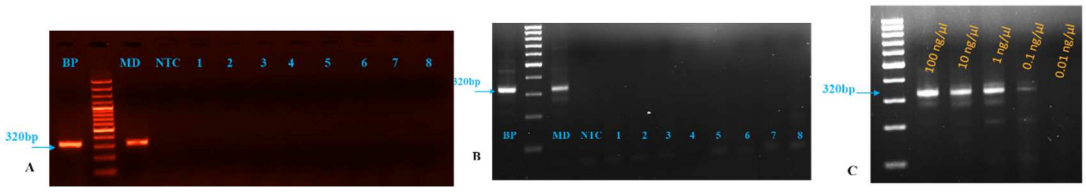

Figure 19: Agarose gel electrophoresis result of the RPA technique specificity and sensitivity.100bp ladder used. A: Single-species PCR; B: RPA; 1-8: positive control templates from Moredun; C: RPA analytical sensitivity test using 10-fold serial dilution control template. BP and MD: positive control; NTC: non-template control

3.6.3 Farm sample trial of RPA

Three out of the five farms tested, namely F-1, F-2 and F-5, gave positive results for the presence of *H. contortus* DNA, while the remaining two farms, F-3 and F-4 gave negative results (Figure 20-B). This was also confirmed by the ITS2 species identification PCR (Figure 20-A). It should be noted that farm F3 (mean EPG = 5.76) with insignificant trichostrongyle egg counts, while F4 had no detectable trichostrongyle egg counts. Furthermore, these results were in agreement with those obtained for the same farms with the ITS2 PCR (Figure 2). This shows that our assay is robust and can accurately and specifically detect *H. contortus* in farm isolates. Although the sensitivity is lower than that described by WU et al. (2021), this nevertheless demonstrates that the RPA assay developed herein offers a comparable detection accuracy to that of the ITS2 species identification PCR in practice for Hungarian field isolates.

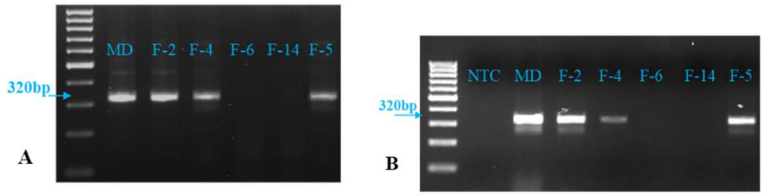

Figure 20: RPA farm trials. 100bp used. A: ITS2 PCR; B: RPA results using arbitrarily selected farm samples (F-2, F-4, F-6, F-5 and F-14).

3.6.4 RPA detection using DNA-intercalating dye.

Preliminary findings showed that after (dye: amplicon ratio) optimisation, RPA amplicons could not be visualised under white light but could be easily detected using a UV light source (Figure 21). The EvaGreen® dye showed promising results in this preliminary trial as the change in colours of the tested RPA tubes was visualised clearly under UV illumination (Figure 21-A). Nevertheless, it should also be noted that the EvaGreen® dye used here was of a low concentration (5x) and this might have also contributed to the failure of any colourimetric change detection by unaided eyes.

The use of a handheld UV lamp of decent quality can easily offset the need for UV illumination to detect any colourimetric change. GelRed™ dye showed inconsistent results; at a working concentration of 10x, the GelRed™ dye correctly illuminated two of three positive control templates under UV (Figure 21-B). This could be due to the mismatched dye-to-amplicon ratio or interference by the RPA reagents. The attempts to rectify and improve this using various working concentrations (100x, 200x and 300x) proved unsuccessful (Figure 21-B), resulting in no change in the colour of the tubes either in white light or UV illumination. Hence, the study acknowledges further work is necessary for this detection system to be fully optimised for an effective farm-side detection system. Despite this setback, these results constitute an important first step towards developing naked-eye detection of RPA amplicons.

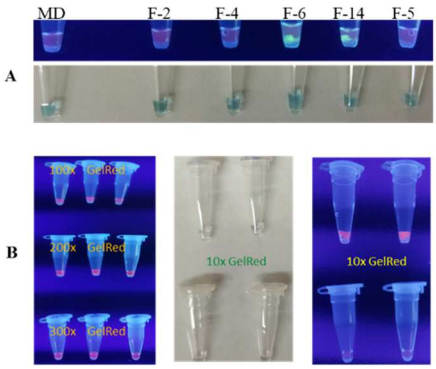

Figure 21: Colourimetric detection of RPA assay results using various DNA intercalating dyes. A: Results of various farms as observed under UV-illumination (upper panel; positive results=purplish-green colour) and white light (lower panel) using EvaGreen® dye; B: Results detected using various concentrations of GelRed dye. The middle panel shows results under white light with no significant colourimetric change. Positive result= purple glow; MD= positive control; F-2, F-4, F-5, F-6 and F-14 = farm samples.

3.6.5 Gene sequencing and phylogenetic analysis: a brief report

The evolutionary history was inferred using the Neighbor-Joining method (SAITOU and NEI, 1987). The optimal tree is shown in Figure 27. The tree presented here (Figure 22) shows 4 clades and 1 outgroup (*H. placei*). Clade-1 (as read from the top-down sequence), consisted of two sequences from Nigeria and Australia with relatively very strong support (bootstrap =100%); clade-2 consisted of isolates from Hungary with good nodal support (bootstrap>50%). In the middle is a cluster comprising many isolates from various parts of the world (bootstrap >85%) while the last one consisted of sequences from Sweden, New Zealand and an *H. longistipes* sequence. The presented phylogenetic tree analysis showed that there is a distinctive haplotype of *H.*

contortus isolates the three farm locations in Hungary. These were evidently at distant places from the outgroup *H. placei* in the tree which is the most closely related species. The finding also agrees with studies in Pakistan (QAMAR et al., 2022), Egypt (KANDIL et al., 2017) and Tunisia (AKKARI et al., 2013) targeting the ITS2 region of *H. contortus*. Closer to Hungary's perspective, a study in Sweden was conducted by TROELL (2006) by comparing the genetic differences in the ITS1 and ITS2 using the *Haemonchus* spp from Sweden and Kenya. It concluded that they could be of the same species but of a distinct population. The study here also presented a common root for the isolates in Kenya, India, Iran, Japan, the USA and China.

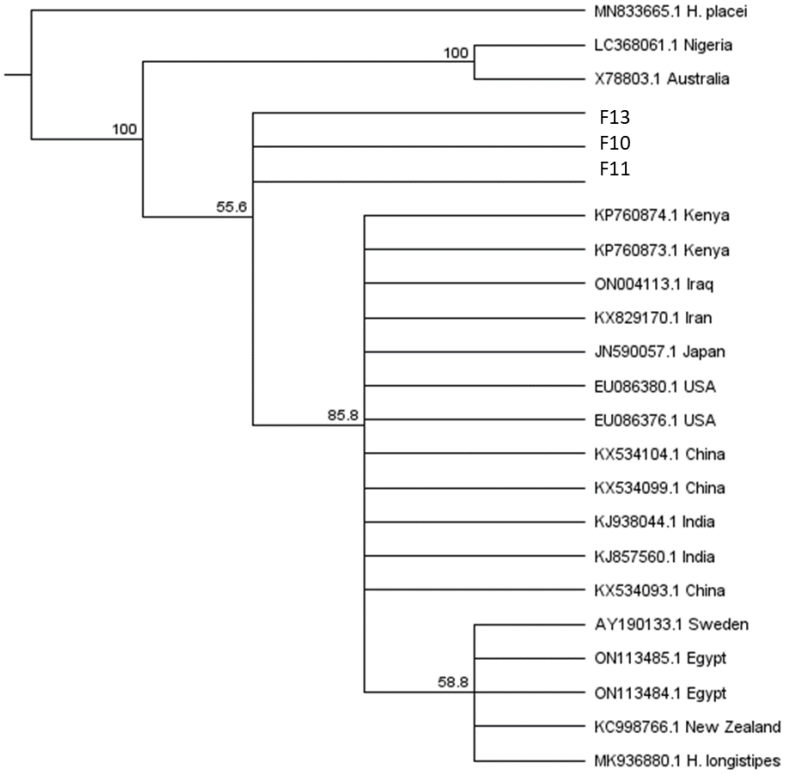

Figure 22: Phylogenetic tree of three *H. contortus* isolates from Hungary as deduced from the ITS2 target region. Bootstrap values >50% are displayed at the nodes. *H. placei* (accession number MN833665) is used as an outgroup.

4 NEW SCIENTIFIC RESULTS

1. A centrifuge-free crude DNA extraction method was successfully adapted using the Fill-FLOTAC apparatus, a magnetic beads DNA extraction kit and a motorised micropestle for egg disintegration.
2. A LAMP and another LAMP-LF assay for the qualitative detection of *H. contortus* from the faecal samples of ruminant flocks were successfully designed. These two assays allow visual detection to the unaided eyes without compromising the specificity and sensitivity. The analytical sensitivity is determined to be 2.5 x 10^{-4} ng/µl of DNA template.
3. An RPA technique, another isothermal-based amplification tool, was also successfully designed for the detection of *H. contortus* with an analytical sensitivity of 0.1 ng/µl DNA template. This study also would like to register two preliminary findings: i) that the post-amplification clean-up for the RPA amplicons could be eliminated without any significant loss in analytical sensitivity, and ii) a colourimetric change detection using some commonly DNA intercalating dyes (such as Eva Green and SYBR Green dyes) is possible.
4. 12 sheep farms and 1 goat farm in 6 counties of Hungary were confirmed to have the *H. contortus* parasite. Recovery of adult worms from the abomasum of hunted roe deers (n>20) and the subsequent molecular-technique-based confirmation of *H. contortus* from the Biharugra village suggested a probable cross-contamination of pasture ground shared between the wild and domestic small ruminants in that area.

5 RESULTS APPLICABLE IN PRACTICE

1. Since a quick and reliable qualitative diagnosis of *H. contortus* can be made without compromising the integrity of the test, a more detailed epidemiological survey can be followed up after such a preliminary screening of selected/suspected farms. This screening can be done side by side with a detailed FEC examination of the farm to present more concise and meaningful data on the occurrence of the important GIT parasites in Hungary, of which the data is very limited at the moment.
2. Need for a study to determine the genetic makeup of the *H. contortus* isolates recovered from both domesticated flocks as well as wild ruminants can be done. This could contribute to reducing the knowledge gap on the genetic characteristics and the diversity of this parasite in Europe in general and Hungary in particular.
3. Mini-FLOTAC system can be effectively integrated into a farm site-friendly nucleic acid amplification detection diagnostic tool, starting from a crude DNA extraction to supplementation of reliable FEC data. Such a combination of the FEC tool and molecular detection of the parasite can be a step towards a clinically significant point-of-care diagnosis that can indirectly help in making an effective deworming decision.
4. Isothermal techniques like LAMP and RPA should be encouraged for veterinary helminth diagnosis considering that isothermal nucleic acid amplification has the advantage of a quick result time without compromising the sensitivity and specificity. Also, there are plenty of assays based on these techniques for the detection of various pathogens including parasites in human medicine either at the field level or in laboratory applications.
5. Currently, there is only a single kit manufacturer for the RPA technique and at the time of writing this, the kit that can use an LF detection system has been discontinued. Accordingly, using a DNA intercalating dye can, to some extent, facilitate a colourimetric detection of results without having to rely on the gel electrophoresis method.

6 REFERENCES

1. ABBAS, I. and HILDRETH, M. (2019). Egg autofluorescence and options for detecting peanut agglutinin binding for the identification of Haemonchus contortus eggs in fecal samples. *Veterinary Parasitology*, *267*, 69–74. https://doi.org/10.1016/j.vetpar.2019.01.009
2. AKKARI, H. – JEBALI, J. – GHARBI, M. MHADHBI, M., – AWADI, S., and DARGHOUTH, M. A. (2013). Epidemiological study of sympatric Haemonchus species and genetic characterization of Haemonchus contortus in domestic ruminants in Tunisia. *Veterinary Parasitology*, *193*(1–3), 118–125.
3. AMARANTE, A. F. T.. (2011). Why is it important to correctly identify Haemonchus species? *Revista Brasileira de Parasitologia Veterinária*, *20*, 263–268.
4. AWAWDEH, L. – TURNI, C. – HENNING, J. – ALLAVENA, R. E. – COBBOLD, R. N., MOLLINGER, J. L., and GIBSON, J. S. (2019). An optimized protocol for molecular screening of avian pathogenic Escherichia Coli from broiler chickens in South East Queensland, Australia. *Journal of Applied Poultry Research*, *28*(4), 1370–1381.
5. BESIER, R. B. – KAHN, L. P. – SARGISON, N. D., and VAN WYK, J. A. (2016). The Pathophysiology, Ecology and Epidemiology of Haemonchus contortus Infection in Small Ruminants. *Advances in Parasitology*, *93*, 95–143. https://doi.org/10.1016/bs.apar.2016.02.022
6. COLDITZ, I. G. – Le JAMBRE, L. F. and HOSSE, R. (2002). Use of lectin binding characteristics to identify gastrointestinal parasite eggs in faeces. *Veterinary Parasitology*, *105*(3), 219–227.
7. CRINGOLI, G. – RINALDI, L. – MAURELLI, M. P. and UTZINGER, J. (2010). FLOTAC: new multivalent techniques for qualitative and quantitative copromicroscopic diagnosis of parasites in animals and humans. *Nature Protocols*, *5*(3), 503–515.
8. DOUANNE, N. – WAGNER, V. – BÉLANGER, D. – FERNANDEZ-PRADA, C. (2019). High-throughput identification and quantification of Haemonchus contortus in fecal samples. *Veterinary Parasitology*, *265*, 24–28.
9. EMERY, D. L. – HUNT, P. W. – LE JAMBRE, L. F. (2016). Haemonchus contortus: the then and now, and where to from here? *International Journal for Parasitology*, *46*(12), 755–769. https://doi.org/10.1016/j.ijpara.2016.07.001
10. FRANCIS, E. K. and ŠLAPETA, J. (2022). A new diagnostic approach to fast-track and increase the accessibility of gastrointestinal nematode identification from faeces: FECPAKG2 egg nemabiome metabarcoding. *International Journal for Parasitology*, *52*(6), 331–342.
11. GUEVARA, E. E. – FRANKEL, D. C. – RANAIVONASY, J. – RICHARD, A. F. – RATSIRARSON, J. – LAWLER, R. R. and BRADLEY, B. J. (2018). A simple, economical protocol for DNA extraction and amplification where there is no lab. *Conservation Genetics Resources*, *10*(1), 119–125.
12. JURASEK, M. E. – BISHOP-STEWART, J. K. – STOREY, B. E. – KAPLAN, R. M. and KENT, M. L. (2010). Modification and further evaluation of a fluorescein-labeled peanut agglutinin test for identification of Haemonchus contortus eggs. *Veterinary Parasitology*, *169*(1–2), 209–213. https://doi.org/10.1016/j.vetpar.2009.12.003
13. KANDIL, O. M. – ABDELRAHMAN, K. A. – FAHMY, H. A. – MAHMOUD, M. S. – EL

NAMAKY, A. H. and MILLER, J. E. (2017). Phylogenetic patterns of Haemonchus contortus and related trichostrongylid nematodes isolated from Egyptian sheep. *Journal of Helminthology*, *91*(5), 583–588.

14. KHANGEMBAM, R. – TÓTH, M. – VASS, N. – VÁRADY, M. – CZEGLÉDI, L. – FARKAS, R., and ANTONOPOULOS, A. (2021). Point of care colourimetric and lateral flow LAMP assay for the detection of Haemonchus contortus in ruminant faecal samples. *Parasite*, *28*. https://doi.org/10.1051/parasite/2021078
15. KUMAR, S. – STECHER, G. – Li, M. – Knyaz, C. and Tamura, K. (2018). MEGA X: molecular evolutionary genetics analysis across computing platforms. *Molecular Biology and Evolution*, *35*(6), 1547.
16. LOBATO, I. M. and O'SULLIVAN, C. K. (2018). Recombinase polymerase amplification: Basics, applications and recent advances. *TrAC - Trends in Analytical Chemistry*, *98*, 19–35. https://doi.org/10.1016/j.trac.2017.10.015
17. LUO, G.-C. – YI, T.-T. – JIANG, B. – GUO, X. and ZHANG, G.-Y. (2019). Betaine-assisted recombinase polymerase assay with enhanced specificity. *Analytical Biochemistry*, *575*, 36–39.
18. MELVILLE, L. – KENYON, F. – JAVED, S. – MCELARNEY, I. – DEMELER, J. and SKUCE, P. (2014). Development of a loop-mediated isothermal amplification (LAMP) assay for the sensitive detection of Haemonchus contortus eggs in ovine faecal samples. *Veterinary Parasitology*, *206*(3–4), 308–312. https://doi.org/10.1016/j.vetpar.2014.10.022
19. NICHOLLS, J. and OBENDORF, D. L. (1994). Application of a composite faecal egg count procedure in diagnostic parasitology. *Veterinary Parasitology*, *52*(3–4), 337–342. https://doi.org/10.1016/0304-4017(94)90125-2
20. O'CONNOR, L. J. – WALKDEN-BROWN, S. W. – KAHN, L. P. (2006). Ecology of the free-living stages of major trichostrongylid parasites of sheep. *Veterinary Parasitology*, *142*(1–2), 1–15. https://doi.org/10.1016/j.vetpar.2006.08.035
21. OLIVEIRA, B. B. – VEIGAS, B. and BAPTISTA, P. V. (2021). Isothermal amplification of nucleic acids: the race for the next "gold standard." *Frontiers in Sensors*, *2*, 752600.
22. PALMER, D. G. and MCCOMBE, I. L. (1996). Lectin staining of trichostrongylid nematode eggs of sheep: rapid identification of Haemonchus contortus eggs with peanut agglutinin. *International Journal for Parasitology*, *26*(4), 447–450.
23. PAPADAKIS, G. – PANTAZIS, A. K. – FIKAS, N. – CHATZIIOANNIDOU, S. – TSIAKALOU, V. – MICHAELIDOU, K. – POGKA, V. – MEGARITI, M. – VARDAKI, M. and GIARENTIS, K. (2022). Portable real-time colorimetric LAMP-device for rapid quantitative detection of nucleic acids in crude samples. *Scientific Reports*, *12*(1), 1–15.
24. PARAS, K. L. – GEORGE, M. M. – VIDYASHANKAR, A. N. and KAPLAN, R. M. (2018). Comparison of fecal egg counting methods in four livestock species. *Veterinary Parasitology*, *257*, 21–27.
25. QAMAR, W. – ZAMAN, M. A. – FAHEEM, M. – AHMED, I. – ALI, K. – QAMAR, M. F. – ISHAQ, H. M. and ATIF, F. A. (2022). Molecular Confirmation and Genetic characterization of Haemonchus contortus Isolates at the Nuclear Ribosomal ITS2 Region: First Update from Jhang Region of Pakistan.

Pakistan Veterinary Journal, *42*(2).

26. REDMAN, E. – PACKARD, E. – GRILLO, V. – SMITH, J. – JACKSON, F. and GILLEARD, J. S. (2008). Microsatellite analysis reveals marked genetic differentiation between Haemonchus contortus laboratory isolates and provides a rapid system of genetic fingerprinting. *International Journal for Parasitology*, *38*(1), 111–122. https://doi.org/10.1016/j.ijpara.2007.06.008
27. RINALDI, L. – AMADESI, A. – DUFOURD, E. – BOSCO, A. – GADANHO, M. – LEHEBEL, A. – MAURELLI, M. P. – CHAUVIN, A. – CHARLIER, J. and CRINGOLI, G. (2019). Rapid assessment of faecal egg count and faecal egg count reduction through composite sampling in cattle. *Parasites & Vectors*, *12*(1), 1–8.
28. ROSE, H. – CAMINADE, C. – BOLAJOKO, M. B. – PHELAN, P. – van DIJK, J. – BAYLIS, M. – WILLIAMS, D. and MORGAN, E. R. (2016). Climate-driven changes to the spatio-temporal distribution of the parasitic nematode, Haemonchus contortus, in sheep in Europe. *Global Change Biology*, *22*(3), 1271–1285. https://doi.org/10.1111/gcb.13132
29. SAITOU, N. and NEI, M. (1987). The neighbor-joining method: a new method for reconstructing phylogenetic trees. *Molecular Biology and Evolution*, *4*(4), 406–425.
30. SALLÉ, G., DOYLE, S. R. – CORTET, J. – CABARET, J. – BERRIMAN, M. – HOLROYD, N. and COTTON, J. A. (2019). The global diversity of Haemonchus contortus is shaped by human intervention and climate. *Nature Communications*, *10*(1), 4811. https://doi.org/10.1038/s41467-019-12695-4
31. SHEN, D. D. – WANG, J. F. – ZHANG, D. Y. – PENG, Z. W. – YANG, T. Y. – WANG, Z. D., BOWMAN, D. D. – HOU, Z. J. and LIU, Z. S. (2017). Genetic diversity of Haemonchus contortus isolated from sympatric wild blue sheep (Pseudois nayaur) and sheep in Helan Mountains, China. *Parasites and Vectors*, *10*(1), 1–10. https://doi.org/10.1186/s13071-017-2377-0
32. SOULSBY, E. J. L. (1968). Helminths, arthropods and protozoa of domesticated animals. *Helminths, Arthropods and Protozoa of Domesticated Animals.*
33. SRISRATTAKARN, A. – TIPPAYAWAT, P. – CHANAWONG, A. – TAVICHAKORNTRAKOOL, R. – DADUANG, J. – WONGLAKORN, L. – SOOKSONGSOONTORN, P. and LULITANOND, A. (2020). Direct detection of methicillin-resistant in Staphylococcus spp. in positive blood culture by isothermal recombinase polymerase amplification combined with lateral flow dipstick assay. *World Journal of Microbiology and Biotechnology*, *36*(11), 1–11. https://doi.org/10.1007/s11274-020-02938-8
34. TAYLOR, M. A. – COOP, R. L. and WALL, R. L. (2015). *Veterinary parasitology*. John Wiley & Sons.
35. TROELL, K. (2006). *Genotypic and phenotypic characterization of Haemonchus contortus in Sweden* (Vol. 2006, Issue 2006: 36).
36. WU, Y. D. – WANG, Q. Q. – WANG, M. – ELSHEIKHA, H. M. – YANG, X. – HU, M. – ZHU, X. Q. and XU, M. J. (2021). Development of a lateral flow strip-based recombinase polymerase amplification assay for the detection of haemonchus contortus in goat feces. *Korean Journal of Parasitology*, *59*(2), 167–171. https://doi.org/10.3347/kjp.2021.59.2.167

7 PUBLICATIONS

UNIVERSITY of DEBRECEN

UNIVERSITY AND NATIONAL LIBRARY
UNIVERSITY OF DEBRECEN
H-4002 Egyetem tér 1, Debrecen
Phone: +3652/410-443, email: publikaciok@lib.unideb.hu

Registry number: DEENK/276/2023.PL
Subject: PhD Publication List

Candidate: Rojesh Khangembam
Doctoral School: Doctoral School of Animal Husbandry
MTMT ID: 10065283

List of publications related to the dissertation

Foreign language scientific articles in Hungarian journals (2)

1. **Khangembam, R.**, Tóth, M., Gulyás, G., Czeglédi, L., Vass, N.: Recovery and confirmation of Haemonchus contortus from abomasal contents of roe deer (Capreolus capreolus) in Eastern-Hungary (Biharugra): A diagnostic case study.
   Acta agraria Debreceniensis. 1, 59-62, 2023. ISSN: 1587-1282.
   DOI: https://doi.org/10.34101/ACTAAGRAR/1/12058

2. **Khangembam, R.**, Czeglédi, L., Vass, N.: Routine microscopy examination of faecal samples as a tool for detection of common gastrointestinal parasites: a preliminary report from two Hungarian farms.
   Acta agraria Debreceniensis. 1, 63-66, 2023. ISSN: 1587-1282.
   DOI: http://dx.doi.org/https://doi.org/10.34101/actaagrar/1/12059

Foreign language scientific articles in international journals (3)

3. **Khangembam, R.**, Vass, N., Morrison, A., Melville, L. A., Antonopoulos, A., Czeglédi, L.: Preliminary Results of the Recombinase Polymerase Amplification Technique for the Detection of Haemonchus contortus from Hungarian Field Samples.
   Vet. Parasitol. Epub, 1-20, 2023. ISSN: 0304-4017.
   DOI: https://doi.org/10.1016/j.vetpar.2023.109974
   IF: 2.821 (2021)

4. **Khangembam, R.**, Tóth, M., Vass, N., Várady, M., Czeglédi, L., Farkas, R., Antonopoulos, A.: Point of care colourimetric and lateral flow LAMP assay for the detection of Haemonchus contortus in ruminant faecal samples.
   Parasite. 28, 1-12, 2021. ISSN: 1252-607X.
   DOI: http://dx.doi.org/10.1051/parasite/2021078
   IF: 3.02

5. Tóth, M., **Khangembam, R.**, Farkas, R., Oláh, J., Vass, N., Monori, I.: A case report: sheep endoparasitism dynamics under semi-dry continental climate of Karcag, Hungary.
   Biol. Tvarin. 21 (2), 66-69, 2019. ISSN: 1681-0015.
   DOI: http://dx.doi.org/10.15407/animbiol21.02.066

Foreign language conference proceedings (1)

6. **Khangembam, R.**, Czeglédi, L., Vass, N.: Detection of Haemonchus contortus eggs using peanut agglutinin (PNA) fluorescence microcopy.
In: XXX Jubilee International Congress of the Hungarian Association for Buiatrics. Proceedings, Magyar Buiatrikusok Társasága / Hungarian Association for Buiatrics, Budapest, 221-224, 2023. ISBN: 9786158141321

Foreign language abstracts (3)

7. **Khangembam, R.**, Czeglédi, L., Vass, N., Antonopoulos, A.: Proof of concept recombinase polymerase assay (RPA) for the detection of Haemonchus contortus in ruminants.
In: ICOPA 2022 International Congress of Parasitology Online Abstracts, World Federation of Parasitologists, Copenhagen, 1269, 2022.

8. **Khangembam, R.**, Vass, N.: Loop-mediated Isothermal Amplification (LAMP) as a tool for diagnosis of parasitism: Why it is gaining popularity.
In: XXIV. Tavaszi Szél Konferencia 2021 : Absztraktkötet. Szerk.: Molnár Dániel, Molnár Dóra, Doktoranduszok Országos Szövetsége, Budapest, 87-88, 2021. ISBN: 9786155586996

9. **Khangembam, R.**, Tóth, M., Vass, N., Várady, M., Farkas, R., Antonopoulos, A.: Point of care colourimetric and Lateral Flow-LAMP Assay for the detection of Haemonchus contortus from ruminant faecal samples.
In: 28th International Conference of the World Association for the Advancement of Veterinary Parasitology WAAVP 2021 : Book of Abstracts. Ed.: Grace Mulcahy, World Association for the Advancement of Veterinary Parasitology, Dublin, 178-179, 2021.

List of other publications

Foreign language scientific articles in international journals (1)

10. Xayalath, S., Mujitaba, M. A., Ortega, A. D. S. V., **Khangembam, R.**, Novotniné Dankó, G., Rátky, J.: Effects of birth weight on puberty and the reproductive performance of crossbred Moo Lath x Duroc gilts = A születési súly hatása az ivarérésre és a szaporodásbiológiai teljesítményre keresztezett Moo Lath x Duroc kocasüldőknél.
J. Cent. Eur. Agric. "Accepted by Publisher" (-), 1-11, 2023. ISSN: 1332-9049.

UNIVERSITY AND NATIONAL LIBRARY
UNIVERSITY OF DEBRECEN
H-4002 Egyetem tér 1, Debrecen
Phone: +3652/410-443, email: publikaciok@lib.unideb.hu

Informational/educational articles (1)

11. Oláh, J., Tóth, M., Molnár, A., Jávor, A., **Khangembam, R.**, Egerszegi, I.: Korszerű módszerek alkalmazása cigája tenyészkos jelöltek hústermelő képességének javítására. *Magyar juhászat + kecsketenyésztés. 28* (9), 2-4, 2019. ISSN: 0025-018X.

Total IF of journals (all publications): 5,841
Total IF of journals (publications related to the dissertation): 5,841

The Candidate's publication data submitted to the iDEa Tudóstér have been validated by DEENK on the basis of the Journal Citation Report (Impact Factor) database.

26 June, 2023

DEBRECENI EGYETEM Egyetemi és Nemzeti Könyvtár